

# Analysis of a broadband processing technology applicable to conventional streamer data

Zhengzheng Zhou,<sup>1\*</sup> Milos Cvetkovic,<sup>1</sup> Bing Xu<sup>1</sup> and Philip Fontana<sup>2</sup> provide a case study to show that processing techniques can realize broadband marine seismic results from conventional streamer acquisition data without the need for the emerging built-for-purpose broadband streamer technology.

The vast majority of marine seismic data is acquired with conventional towed streamer cables which are equipped only with hydrophones and are all typically towed at the same constant depth for any single survey. The receiver ghost zeros out the spectral response of the recorded data at notch frequencies equal to any integer divided by the ghost delay time, limiting both the top end of the usable spectrum as well as attenuating the low frequency response. The source ghost has a similar effect. The combined effect of the ghosts results in greatly reduced resolution in the subsurface image. A conventional 'solution' for this problem is to tow the sources and streamers shallow (at less than 7 m of depth below the surface) to obtain higher frequencies at the expense of attenuating low frequencies and exposing the sensors to a noisier environment near the sea surface.

Over the past few years, several distinct technological advances have emerged that make it possible to mitigate the effects of the ghosts and obtain broadband images with greatly enhanced resolution. These methods combine two or more distinct measurements to remove the ghosts. The combinations can be either hydrophone plus geophone (Carlson, 2007), or hydrophones on streamers towed at different depths (Posthumus, 1993), or hydrophones at offset-variable depths (Soubaras, 2010). In each case, the de-ghosting process is not a simple sum of different measurements in x-t domain, but rather it often requires sophisticated processing flows to accomplish. These methods require non-conventional data acquisition, either with streamers equipped with multi-component sensors, or with streamers configured in unconventional geometries such as over-and-under or slanted configurations. Such methods are not applicable to conventional 'flat' streamer data. Therefore, it is beneficial to have a purely processing-based broadband technique that can recover the high frequency data beyond the ghost notches and enhance the low frequency signal attenuated by the ghosts, as such a processing method can greatly extend the resolution of conventional marine seismic data.

We have developed an effective broadband processing method based on a new de-ghosting technique. It can remove

most of the ghost effects from conventional streamer data. In this paper, we will refer to this method as WiBand. It is designed to address both the amplitude attenuation and the phase distortion introduced by the ghosts to obtain nearly flat spectral response in the typical range of 4 Hz to 150 Hz, as well as a compact, well focused seismic wavelet. In order to validate our method, we carried out an experiment in which multiple streamers were towed at different depths and evaluated the phase reconstruction fidelity of the algorithm by comparing the WiBand result from the deep tow data with the standard processing result from the shallow tow data.

It should be noted that there are many other effects that limit the resolution of seismic images such as the absorption and scattering of high frequencies by the earth, the difficulty of removing high frequency multiples, and the difficulty of obtaining a velocity model good enough to focus high frequencies under complex overburden. We will not address these issues here.

## De-ghosting methods

Up-going seismic waves are reflected downward by the sea surface with near -1 reflection coefficient. At any given depth below the surface, the up and down going waves interfere destructively at certain frequencies producing notches in the power spectrum of the data recorded at that depth. There have been many attempts at solving this problem (Robertsson, 2002). The standard operator for removing the receiver ghost is an x-y-t domain pseudo-differential operator:

$$D = \frac{1}{1 + r e^{2iz\sqrt{\omega^2/c^2 - k_x^2 - k_y^2}}}$$

This operator is to be applied to shot records. Here,  $r$  is the surface reflection coefficient which is close to -1;  $c$  is the near surface sound velocity and is close to 1500m/s;  $z$  is the receiver depth. This operator is typically applied in the f-k or f-p domains. However, stable application of this operator is very difficult due to its near singularity, the variability of  $r$  and  $z$ ,

<sup>1</sup> ION GX Technology.

<sup>2</sup> Polarcus.

\* Corresponding author, E-mail: Zheng.Zhou@iongeo.com

## Data Processing

and the difficulty of transforming streamer data into f-k or f-p domain without end point artifacts. For instance, when the streamer depth varies up to  $\pm 1\text{m}$ , this operator is no longer stationary along the cable and additional corrections are required. Furthermore, because the operator is non-linear in the key parameters  $r$  and  $z$ , obtaining these parameters directly from the input data requires effective non-linear optimization methods and carefully selected objective functions (Baan, 2008; Mo, 2009). Nevertheless, the advantage is that the operator is described by a very small set of variables that makes such non-linear problems solvable. Typically, only a 2D version of this operator can be applied.

Another line of attack on the de-ghosting problem uses variations of traditional blind deconvolution methods (Zhang, 2011). In order to overcome the mixed phase nature of ghosted data, the L2-norm objective function of standard Weiner-Robinson deconvolution must be replaced with non-quadrilinear measures. A subtle difficulty with this approach is that the convolutional operators required are fairly long when expressed in the time domain, so a direct time domain approach to solve the non-linear optimization problem faces the issue of a large number of degrees of freedom. This approach also requires special techniques to extend its application to earth models that are not one-dimensional.

The WiBand workflow combines the strengths of these two types of de-ghosting approaches, and data-adaptively derives the most stable operator to remove the effects of the source and receiver ghosts from the data prior to migration. As such, it is not a data creation method, but a method to recover the signal weakened by the ghosts and relies on the presence of usable signal at and near the ghost frequencies in the raw data.

Figures 1(a) and (b) compare a standard processing result (a) with a WiBand result (b) from an offshore Gabon dataset acquired in 2011 using a streamer towed at 15 m below sea surface. The receiver ghost notch associated with this depth is about 50 Hz and in the standard processing flow a high-cut filter was applied to remove energy above 55 Hz from the data. No high-cut filtering was applied in the WiBand processing flow. It is apparent from this comparison that the WiBand flow has managed to greatly enhance the resolution of the image. Both low and high frequency signals have been enhanced and many structural details invisible in the standard product are well resolved in the WiBand image.

### Deep tow versus shallow tow test

In order to validate the WiBand results, we need to closely examine the phase of the WiBand output, particularly the phase of the high frequency part of the signal above the first receiver ghost notch frequency. One way of performing this analysis is to compare WiBand output from a deep tow dataset with a raw shallow tow dataset which has near zero-phase signal beyond the ghost notch of the deep tow data.

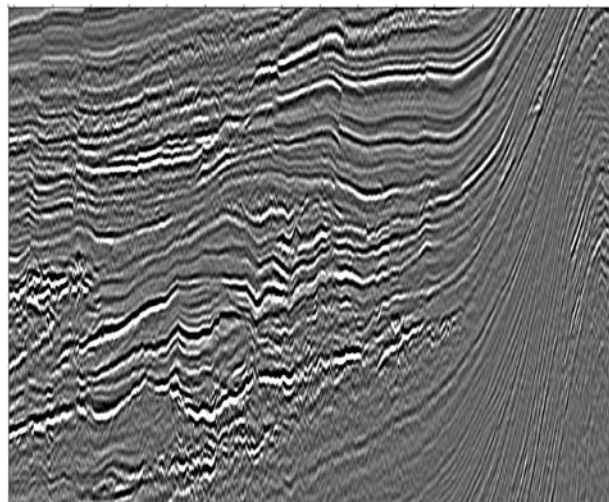


Figure 1(a) Standard 4 ms PSTM image.

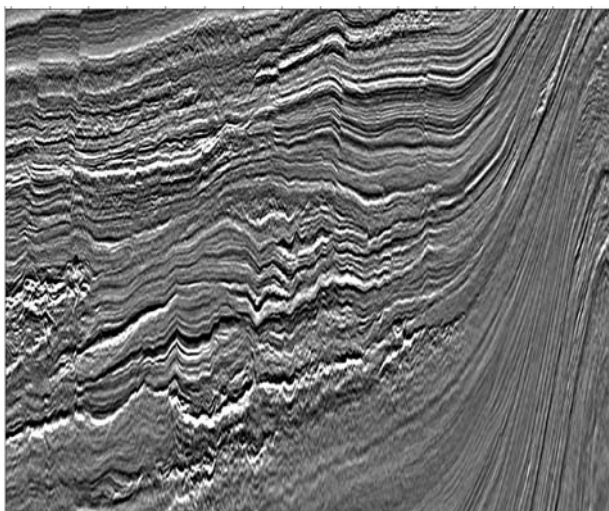


Figure 1(b) WiBand 2 ms PSTM image.

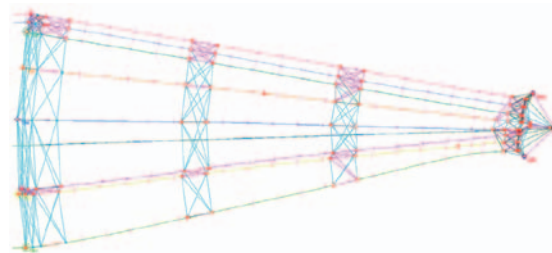


Figure 2 Streamers were towed in a fan pattern. The blue line just above the dark green line represents streamer 4 (deep tow). The orange line above streamer 4 represents streamer 5 (shallow tow).

For this purpose, we acquired a new dataset in 2012 in the same general area offshore Gabon. In this new experiment, eight streamers equipped with lateral position controllers were deployed in a fan pattern (Figure 2) and towed at different depths. Two air gun arrays were towed at different depths and were fired in alternating order. For

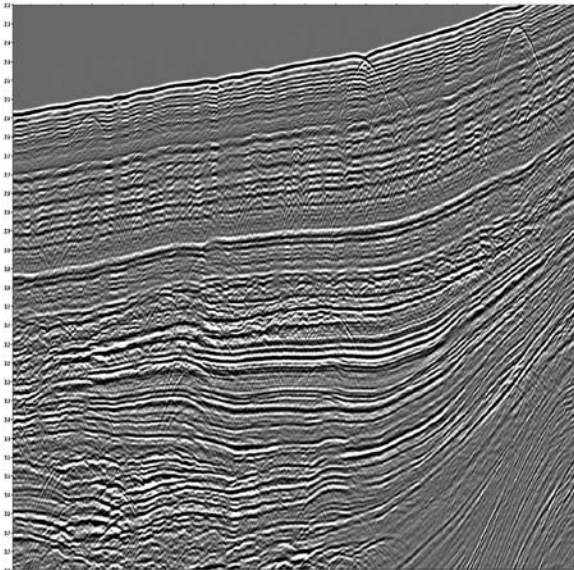


Figure 3(a) Shallow tow data raw stack.

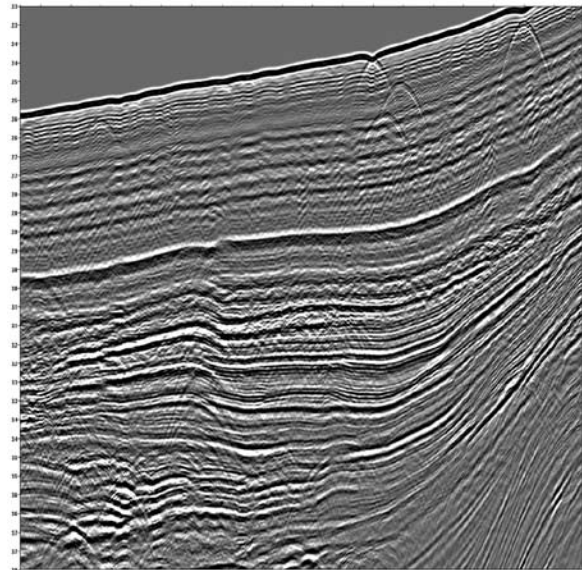


Figure 3(b) Deep tow data raw stack.

this paper, we focus on the data associated with the 5 m source and recorded by the two central streamers, which are streamer 4, towed at 12 m depth, and streamer 5, towed at 7 m depth. We refer to streamer 4 data as the deep tow line and streamer 5 data as the shallow tow line.

As can be observed from Figure 2, streamer 5 has a much larger feathering angle relative to the sailing direction than streamer 4. This feathering results in considerable mid-point dispersal when we bin the data according to nominal 2D geometry. Therefore, for the purpose of comparing the two lines, we focus on the first second or so of data below the water bottom. For the shallow tow line, the extent of mid-point dispersal within a single CDP bin is about 200 m over the range of offsets contributing to the stack at the water bottom level. For the deep tow line, the relevant dispersal extent is 50 m. For the same CDP bin, the average midpoint locations for the two lines are about 200 m apart.

In Figures 3(a) and (b), we show the raw stacks from the shallow tow line (a) and the deep tow line (b). The two sections display dramatically different wavelet characteristics. This difference stems from the different ghost delays in the two datasets. Notice the dramatic difference in the seismic wavelet in these two sections. Figure 4 shows the effect of a ghost on the amplitude and phase of recorded data. The ghost introduces notch frequencies at which the amplitude is greatly attenuated due to destructive interference. More importantly, across each of these notch frequencies, the phase response undergoes a rapid 180° degree rotation, putting the data beyond the first notch in opposite polarity to the main band of data below that notch.

In our case, the deep tow data has a notch and a polarity flip at 63 Hz which is very close to the peak frequency of the shallow tow data (see Figure 6), leading to the dramatic difference in the appearance of the two sections. It is therefore

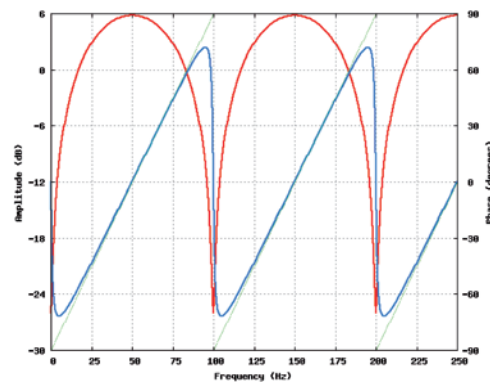


Figure 4 Phase (blue) and amplitude (red) spectra of the operator representing a ghost at 10 ms delay with a -0.95 surface reflection coefficient.

very instructive to use the shallow tow data as a standard to analyze the phase characteristics of the WiBand result from the deep tow data.

### Analysis of results

We first compare the WiBand results from both datasets. It is apparent from Figures 5(a) and (b) that, after WiBand, the two datasets are no longer dramatically different in their wavelet characteristics. The spectral plots in Figure 6 shows that the WiBand process has largely filled in the ghost notches in the power spectra, and the resultant power spectra from both the deep and the shallow tow data have similar spectral slope over a very broad frequency range. Because the WiBand process is applied independently to these two lines, the common spectral shape post-WiBand suggests that the de-ghosting process worked in a consistent fashion.

To analyze the phase fidelity of the WiBand result, we will use the 5–105 Hz band of the raw shallow tow data as

# Data Processing

the standard, as we know from Figure 4 that the shallow data has essentially linear phase within this band modulo phase of the source wavelet, which is common to both the

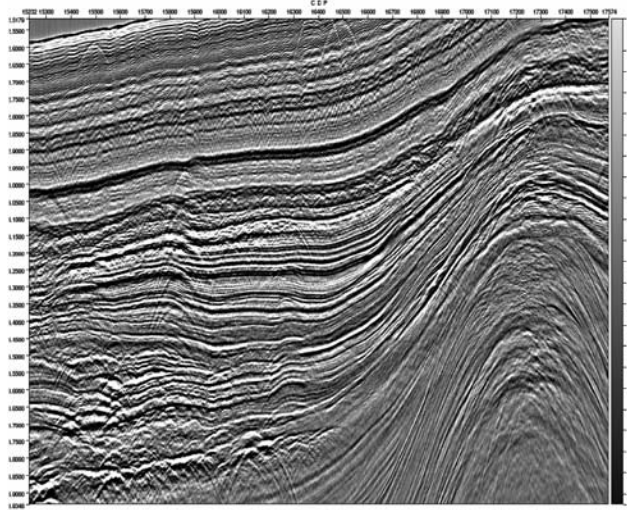


Figure 5(a) WiBand result from the shallow tow line.

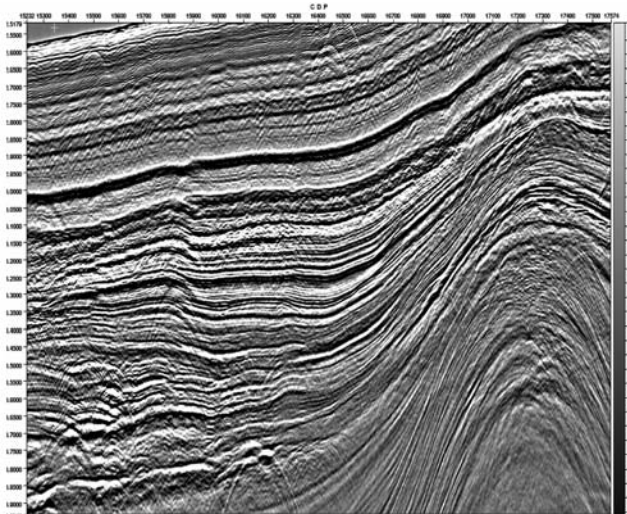


Figure 5(b) WiBand result from the deep tow line.

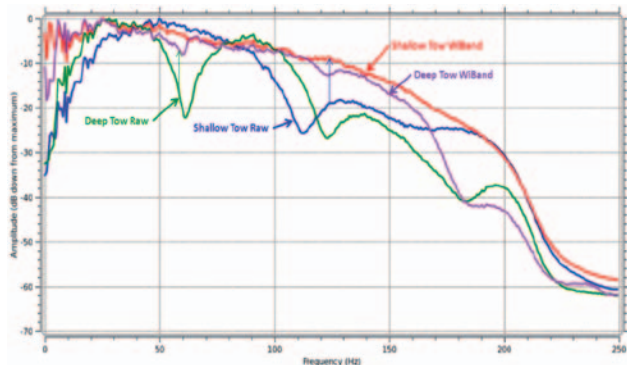


Figure 6 Spectra of the deep tow and shallow tow datasets before and after WiBand processing.

shallow and the deep tow lines. So if the WiBand result from the deep tow line matches in phase the raw shallow tow data in this band, we can conclude that the WiBand process has correctly reversed the deep tow data's polarity flip at 63 Hz.

In order to use the shallow tow data as the standard, we first apply a zero-phase high-cut filter to it to remove the phased-distorted part of its signal beyond its notch frequency of 110 Hz. The power spectra of the shallow tow data before and after this filter are plotted as the blue and red curves in Figure 7. To focus on the phase characteristics of the deep tow WiBand results when comparing it to the filtered shallow tow data, we apply a zero-phase shaping filter to match its power spectrum to that of the filtered shallow tow data. The spectra of the deep tow WiBand data before and after this shape-filtering are plotted as the green and purple curves in Figure 7.

We display the high-cut filtered shallow tow data in Figure 8, and the shape-filtered deep tow WiBand data in Figure 9. By comparing Figures 8 and 9, we determine that the two images match well in phase. That we do not obtain perfect match can be attributed to the disparities in the feathering geometries of the two lines discussed earlier.

In Figure 10, we plot two traces, one from each line, from the marked locations in Figures 8 and 9. The traces have the afore-mentioned filters applied. A very good match is observed between the two traces. The peaks and troughs of the major reflection events line up very well. In particular, the phases of the main events match remarkably well considering distance between the two lines (indeed, some of the minor mismatches can be attributed to diffractions which occur at different locations in these two lines.) For the deep tow WiBand trace displayed here, the recovered signal around the ghost notch at 63 Hz contributes very significantly to its waveform. Therefore, a good match to the shallow tow data cannot be obtained unless the phase of the recovered signal near and above the notch frequency has been reconstructed correctly by the WiBand process.

### Signal-to-noise ratio of raw data

In order for any de-ghosting process to work properly and recover useful signal at and beyond the ghost notch, the raw

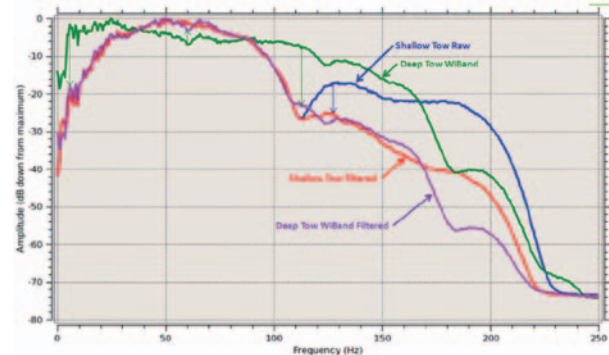


Figure 7 Spectra of the shallow tow data, raw in blue and after zero-phase high-cut filtering in red, and spectra of the deep tow WiBand data in green, and after zero-phase shaper-filtering in purple.

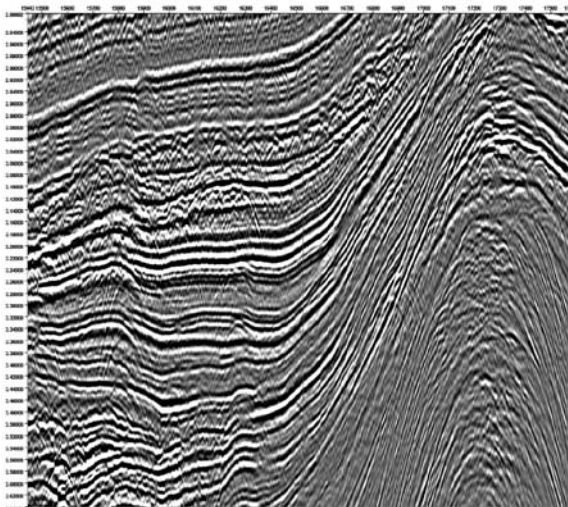


Figure 8 Raw shallow tow data with only a zero-phase high-cut filter to remove energy above its receiver notch frequency of 110 Hz.

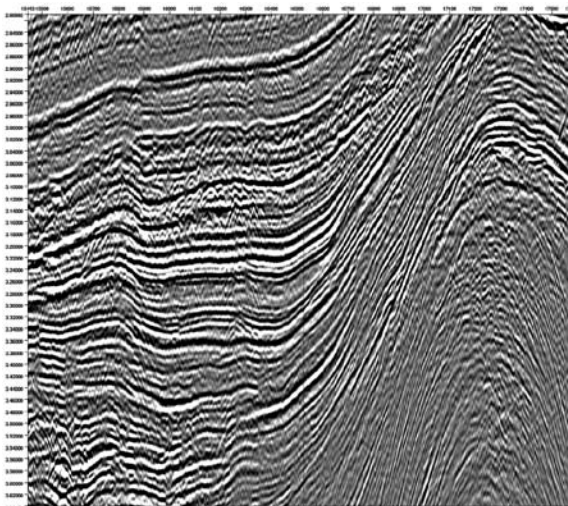


Figure 9 WiBand result from the deep tow data with zero-phase shaping filter to match its power spectrum to the data in Figure 8.

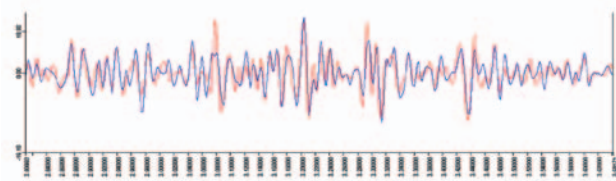


Figure 10 Central traces from sections in Figures 8 (red) and 9 (blue).

data must have useful signal at and around the notch frequency. It is our view that modern marine streamer acquisition equipment has advanced sufficiently so that the various modes of streamer-borne noises are much lower than even the very weak signal present at the notch frequencies.

In Figure 11, we plot signal and noise spectra of the data recorded by the first channels from the shallow tow cable at 7 m depth and the deep tow cable at 12m depth. The noise

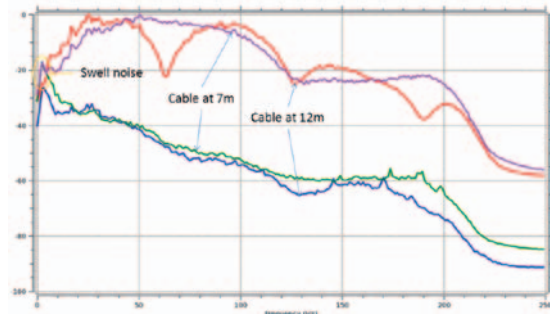


Figure 11 Signal and noise spectra of raw single channel sections.

spectra are measured from a 600 ms data window below direct arrivals and above water bottom reflections. The signal spectra are taken from a 600 ms data window that starts 600 ms below the water bottom reflection. The source volume is 2950 cu in. The noise above 20 Hz is well below the signal strength, even for ghost notch frequencies. This supports our view that the raw data inherently supports de-ghosting.

Also worth noting is that the higher-frequency noise above 20 Hz is dominated by streamer-born modes and towing depth has little impact on them, whereas the tow depth does strongly influence the strength of the swell noise the receivers are exposed to. To avoid the swell noise, one would wish to tow the streamers very deep; however, too great a towing depth would mean that the first-order receiver ghost would be pushed lower and closer to the dominant frequency of the streamer-born noise, which is not reduced by the deeper towing, reducing the signal-to-noise ratio at the notch frequency and limiting the ability of processing-based solutions to recover that data near the notch frequency. This analysis suggests that one should measure the relative strengths of the swell noise and the streamer-borne noises if possible and design the survey parameters to optimize the signal-to-noise ratio over the whole target frequency range.

**Conclusion and discussion**

We have successfully recovered broadband signal from deep tow streamer data and obtained high-resolution images. For the deep tow data, the prominent receiver ghost notch at 63 Hz is filled. An essentially flat power spectrum is recovered between 4 Hz and 150 Hz. We have validated the result by comparing it to shallow tow data which is known to have a near-linear-phase wavelet below 110 Hz. The comparison shows that the phase of the recovered broadband data matches that of the shallow tow data indicating that the strong phase distortion at 63 Hz originally present in the deep tow data has been corrected.

We believe that a processing-based broadband solution can provide an effective alternative to the solutions based on acquisition and processing that require non-conventional streamer acquisition. A processing-based solution can be applied to existing conventional streamer data to extract the maximum value out from the data. Much of our current

## Data Processing

datasets have been processed through workflows that start with a resampling to 3 or 4 ms and contain high-cut filters that remove most of the energy above the first order receiver ghost notch frequency. We have demonstrated that there is a great amount of information present in the raw data that is lost through such standard processing flows, and that such information can be retained and utilized through a new type of workflow that carefully preserves all the signal and properly compensates for the effects of the ghosts.

Our method can also be used in the context of new acquisition and remove the constraints on receiver depth posed by the requirements for high frequency signal. Since the ghost notch can be effectively filled, a new acquisition no longer has to have the receivers shallow in order to record frequencies above approximately 90 Hz. Rather, the acquisition parameters can now be chosen to both improve operational efficiency and optimize signal-to-noise ratio over the whole desired frequency band by considering factors such as swell noise and avoiding positioning the ghost notch at a dominant frequency of streamer-borne noise.

## Acknowledgements

We would like to thank Ophir Energy and the government of Gabon for allowing the acquisition of the experimental

data in Ophir's block offshore Gabon. We would also like to thank the Polarcus acquisition crew and management for making this experiment possible.

## References

- Baan, M. and Pham, D. [2008] Robust wavelet estimation and blind deconvolution of noisy surface seismics: *Geophysics*, 73(5) V37–V46.
- Carlson, D. [2007] Increased resolution of seismic data from a dual sensor streamer cable. *76<sup>th</sup> SEG Annual International Meeting*, Expanded Abstracts.
- Fontana, P., Cheriyan, T. and Saxton, L. [2011] Why not narrowband. *81<sup>st</sup> SEG Annual International Meeting*, Expanded Abstracts.
- Posthumus, B. J. [1993] Deghosting using a twin streamer configuration. *Geophysical Prospecting*, 41, 267–286.
- Robertsson, J. and Kragh, E. 2002, Rough-sea deghosting using a single streamer and a pressure gradient approximation: *Geophysics*, 67(6), 2005–2011.
- Soubaras, R. [2010] Deghosting by joint deconvolution of a migration and a mirror migration. *80<sup>th</sup> SEG Annual International Meeting*, Expanded Abstracts, 3406–3410.
- Zhang, Y. and J. Claerbout, 2011, A new bidirectional deconvolution method that overcomes the minimum phase assumption: Stanford Exploration Project Report No. 142.

Don't forget,  
it's time to...

# Renew your EAGE membership for 2013

Pay before 31 December 2012 and continue receiving the following benefits:



### First Break

A new issue of *First Break* every month. Discount on additional EAGE journals.



### Attractive bookshop offers

EAGE members get attractive discount on books from the EAGE (online) Bookshop. Visit [www.eage.org/bookshop](http://www.eage.org/bookshop) for more information.

### Discount on events

Benefit from discount on all EAGE events worldwide. EAGE's Annual conference & exhibition will take place in London (UK), from 10-13 June 2013.



### Access to EarthDoc

Unlimited access to EAGE's online geoscience database with around 45,000 event papers and scientific articles.



### Renew online via [www.eage.org](http://www.eage.org)!

- Step 1** Go to [www.eage.org](http://www.eage.org) - Login to My Account  
**Step 2** Log in with your membership number (or login name) and password  
**Step 3** Click on My EAGE, then select 'My Services - Renew Membership'

EAGE online services: easy, fast and secure

More benefits?  
Visit our website: [www.eage.org](http://www.eage.org)

# EAGE